Original article

Modelling the effect of food depletion on scallop growth in Sungo Bay (China)

Cédric Bacher [a],*, Jon Grant [b], Anthony J.S. Hawkins [c], Jianguang Fang [d], Mingyuan Zhu [e], Mélanie Besnard [a]

[a] *Ifremer, Crema, BP 5, 17137 L'Houmeau, France*
[b] *Department of Oceanography, Dalhousie University, 1355 Oxford Street, Halifax, NS, Canada B3H 4J1*
[c] *Plymouth Marine Laboratory, Prospect Place, Plymouth PL1 3DH, UK*
[d] *Chinese Academy of Fishery Sciences, 106 Nanjing Road, 266071 Qingdao, People's Republic of China*
[e] *SOA-FIO, Xianxialing Road, Hi-Tech Industrial Park, 266061 Qingdao, People's Republic of China*

Abstract

Sungo Bay (China) has a mean depth of 10 m, a total area of 140 km^2 and is occupied by several types of aquaculture, whilst opening to the ocean. The production of scallops (*Chlamys farreri*) cultured on long lines is estimated to exceed 50 000 tonnes (total weight) per year. Selection of sites for scallop growth and determination of suitable rearing densities have become important issues. In this study, we focused on the local scale (e.g. 1000 m) where rearing density, food concentration and hydrodynamics interact. We have developed a depletion model coupling a detailed model of *C. farreri* feeding and growth and a one-dimensional horizontal transport equation. The model was applied to assess the effect of some environmental parameters (e.g. food availability, temperature, hydrodynamism) and spatial variability on growth, and to assess the effect of density according to a wide range of hydrodynamical and environmental conditions. In the simulations, food concentrations always enabled a substantial weight increase with a final weight above 1.5 g dry weight. Compared to a reference situation without depletion, a density of 50 ind m^{-3} decreased growth between 0% and 100%, depending on current velocity when maximum current velocity was below 20 cm s^{-1}. The mean ratio between food available inside and outside the cultivated area (depletion factor) varied with the percentage of variation in scallop growth that was due to density. Our model suggests that scallop growth was correlated with maximum current velocity for a given density and current velocity below 20 cm s^{-1}. The model was integrated within a Geographical Information System (GIS) to assist in making decisions related to appropriate scallop densities suitable for aquaculture at different locations throughout the bay. Concepts (depletion), methods (coupling hydrodynamics and growth models), and the underlying framework (GIS) are all generic, and can be applied to different sites and ecosystems where local interactions must be taken into account.

Résumé

Modélisation de l'effet de la diminution de nourriture sur la croissance du pétoncle dans la baie de Sungo (Chine). La baie de Sungo (Chine) est une baie largement ouverte sur l'océan, qui occupe une surface de 140 km^2 pour une profondeur moyenne de 10 m et dont une grande partie est consacrée à l'aquaculture. La production annuelle de pétoncles (*Chlamys farreri*) dépasse ainsi les 50 000 tonnes (poids total). La sélection de sites et la définition de densité d'élevage favorables à la croissance sont devenues un enjeu important. Nous avons développé un modèle mathématique prenant en compte les interactions entre densité d'élevage, concentration de nourriture et hydrodynamisme à un niveau local, défini par une distance typique de 1000 m, afin de prédire la diminution de nourriture liée à la consommation par les pétoncles (appelée par la suite « déplétion ») et son effet sur la croissance. Ce modèle s'appuie d'une part sur des équations détaillant la nutrition et la croissance du pétoncle et d'autre part sur un modèle de transport horizontal unidimensionnel. Il permet d'évaluer l'effet des conditions environnementales (nourriture, température, hydrodynamisme) et de leur variabilité spatiale sur la croissance et de tester l'influence de la densité d'élevage pour ces différentes conditions. Nous avons comparé une situation sans déplétion (où la croissance est maximale) à une situation avec une densité d'élevage de 50 ind par m^3. Le modèle indique des diminutions de croissance entre 0 et 100 % en fonction de la vitesse du courant tant que la vitesse maximale reste en dessous de 20 cm s^{-1}. Cette variation de croissance annuelle peut être mise en relation

* Corresponding author.
E-mail address: cbacher@ifremer.fr (C. Bacher).

avec le rapport entre la concentration moyenne de nourriture à l'intérieur et à l'extérieur du domaine cultivé, qui est un indice de déplétion reflétant principalement l'effet de la vitesse du courant. Le modèle a été intégré à un Système d'Informations Géographiques (SIG) ce qui permet de simuler et cartographier rapidement et automatiquement la croissance annuelle et de fournir ainsi des recommandations sur la densité d'élevage appropriée. Le concept de déplétion, le couplage d'un modèle de croissance et d'un modèle hydrodynamique et l'utilisation d'un SIG sont transposables à d'autres systèmes comparables dans lesquels les interactions locales doivent être considérées.

1. Introduction

The development of shellfish aquaculture raises questions regarding its sustainability defined via the carrying capacity concept, i.e. the maximum production achievable in a given ecosystem given the biological constraints and characteristics of the aquaculture activity. Assessment of the maximum yield is relevant if one considers that little was known until recently on regarding the capacity of ecosystems to support aquaculture activity apart from some empirical knowledge or successful/unsuccessful trials to adapt different species in coastal areas. Since shellfish production is an important component of the fisheries resources of coastal communities, carrying capacity assessment has become a major focus of scientific studies facilitating coastal zone management.

These topics are of particular importance in China where traditional aquaculture has been ongoing for centuries, but has been undergoing especially rapid growth in the past 10 years (Guo et al., 1999). Coastal zone management in China has become a major concern because of the following reasons: (i) the impact of human activities on environmental and water quality, and (ii) the need for optimization of aquaculture strategy (Fang et al., 1996). Within this context, a project was funded by the European Union to build tools capable of characterizing the carrying capacity and impact of shellfish and kelp aquaculture in two Chinese bays situated in Shandong province. Cooperative studies were conducted on the feeding responses and growth of cultivated species, variation in key environmental parameters in the field, and modelling hydrodynamics, filter-feeder growth and ecosystem dynamics.

When addressing carrying capacity assessment, an important first step is to describe and quantify the relationship between filter-feeders and the environment, considering eco-physiological processes such as food filtration, ingestion, assimilation and metabolic losses (Dame, 1993). Physiological processes are driven by temperature, food concentration (particulate organic matter (POM), phytoplankton) flow and total suspended matter concentration which act on the ability of the individual to ingest or to reject a fraction of the available food as pseudofaeces. Modelling these processes allows prediction of the relationship between individual scope for growth (SFG) and environmental factors. Ecophysiology models have been published recently for *Mytilus edulis* (Scholten and Smaal, 1998; Grant and Bacher, 1998), *Crassostrea virginica* (Powell et al., 1992), *Crassostrea gi-*

gas (Raillard et al., 1993; Barillé et al., 1997; Ren and Ross, 2001), pearl oyster *Pinctada margaritifera* (Pouvreau et al., 2000), *Tapes philippinarum* (Solidoro et al., 2000), which can be used to identify food limitation. A second step is to define the geographical scale of any food limitation. Carrying capacity may be defined at the ecosystem scale when major parts of the bay are occupied by aquaculture (Raillard and Menesguen, 1994; Dowd, 1997; Bacher et al., 1998; Ferreira et al., 1998). Tidal currents and the geographical position of filter-feeders may also result in a low percentage of food used by those filter-feeders (Grant, 1996), so that investigations at local scales are relevant when rearing density and/or low currents are suspected to influence growth through food depletion (Incze et al., 1981; Pilditch et al., 2001; Pouvreau et al., 2000). An understanding of food limitation in cultured populations assists managers in defining the suitability of sites for aquaculture (Nath et al., 2000).

This paper is one of a series dealing with carrying capacity assessment in Sungo Bay at different spatial scales. Sungo Bay is a small bay with a mean depth of 10 m, total area of 140 km^2, opening to the ocean and occupied by several types of aquaculture, e.g. kelp (*Laminaria laminaria*), oysters (*Crassostrea gigas*) and scallops in lantern nets (*Chlamys farreri*) (Fig. 1). It is one of the most intensively cultured bays in China. The current velocity is driven by the tide and is usually <20 cm s^{-1}. Due to low nutrient inputs from rivers,
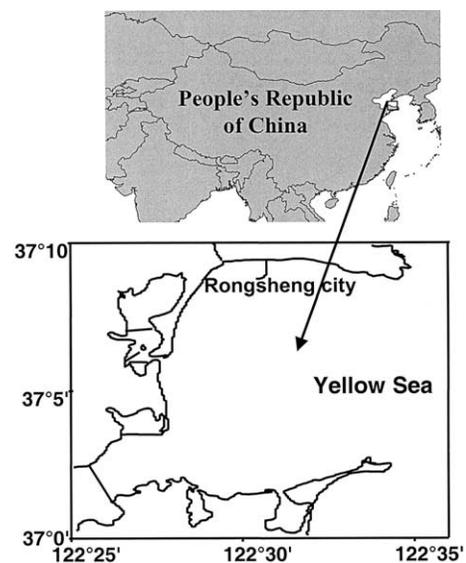
Fig. 1. Location of Sungo Bay (China).
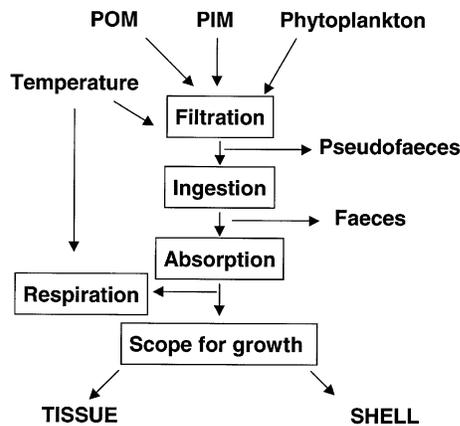
Fig. 2. Conceptual scheme of the scallop feeding and growth model (from Hawkins et al., 2002). Food sources are POM and phytoplankton. Physiology functions also depend on temperature and PIM. Filtration, ingestion, pseudofaeces and faeces production are computed for POM, PIM and phytoplankton (see Table 1 for details).

primary production originates from the import of organic matter and nutrients from the sea, including recycling of nitrogen within the bay. The total production and standing stocks have changed over the past 20 years, including a shift from kelp to shellfish production. However, overexploitation is apparent from reduced shellfish growth and the increased incidence of disease. Scallops are the dominant cultivated filter-feeders, and production is estimated as ~50 000 tonnes (total weight) per year. Selection of sites favourable for scallop growth, and determination of suitable rearing densities have become important issues. We focus here on the local scale where rearing density, food concentration and hydrodynamics interact. The first objective was to assess individual scallop growth by combining a hydrodynamic model to predict current velocity and food delivery (Grant and Bacher, 2001) with an ecophysiological model to predict responsive adjustments in scallop feeding and growth (Fig. 2) (Hawkins et al., 2002), taking into account any food depletion. The combined "depletion model" was used to simulate individual growth at several sites where food concentration had been measured, determining the sensitivity of annual growth to scallop density. The second objective was to integrate the model within a Geographical Information System (GIS) to assist in making decisions about the appropriate densities suitable for aquaculture at different sites throughout Sungo Bay.

2. Methodology

2.1. Depletion model

The depletion model is coupling food transport, food consumption by the scallop population and scallop growth at the scale of a cultivated area—e.g. within a domain of a given length (typically 1000 m). Since we restricted the computations to local scales, we considered the main direction of the current at a given site. The model is based on a one-

dimensional (1D) equation comparable to Pilditch et al. (2001) and Wildish and Kristmanson (1997) when vertical mixing prevents a vertical gradient of particle concentration:

$$\frac{\partial C}{\partial t} + u\frac{\partial C}{\partial x} = N \cdot f(C, w) \qquad (1)$$

where C refers to either phytoplankton, organic or inorganic particulate matter, u is the current velocity, $f(C,w)$ is the individual food consumption, N is scallop density, w is scallop tissue dry weight (DW), x is the distance along the main current direction. Compared to Pilditch et al. (2001), we neglected dispersion terms, since (i) dispersion coefficients are difficult to determine, (ii) their major effect is smoothing the variation inside the domain, and (iii) the numerical integration scheme yields numerical dispersion. Food depletion is related to consumption by animals, which was derived either from the ingestion rate or filtration rate. Filtration rate would indeed modify the particle concentration, but an important fraction of the filtered particles would remain in the water column as pseudofaeces and would be reused by filter-feeders. On the other hand, it could also be argued that these particles would likely sink and therefore would not be available for other animals. This is the reason why we compared two models by calculating depletion due either to filtration or ingestion rate. In both the cases forcing functions and the model of scallop growth were the same (see the following description). When depletion was related to ingestion, food contained in the pseudofaeces was reused with the same efficiency and energy content.

The weight change of the scallop is described by:

$$\frac{dw(x, t)}{dt} = g(C, w, T) \qquad (2)$$

where T is the water temperature and $g(C,w,T)$ is net energy balance established using a model of feeding and growth that has been developed, calibrated and validated for *C. farreri* on the basis of field measurements in Sungo Bay (Hawkins et al., 2002) (refer Table 1 and Fig. 2 for details). In this model, the rates of filtration, ingestion, assimilation and respiration are predicted from the abundances of total particulate matter (TPM), POM and chlorophyll *a*, including seawater temperature. Net energy balance is determined as the difference between rates of assimilation and respiration, and the balance is allocated between somatic tissue, shell and reproduction. Eqs. (1) and (2) above use these functions from the model of Hawkins et al. (2002) to couple food concentration and scallop growth, such that high scallop densities were expected to result in increased food depletion and diminished growth.

Current velocity was predicted by a hydrodynamic model described in Grant and Bacher (2001). This model computes water height and current velocity on an irregular grid of 227 nodes all over the bay, which yields more accurate calculations in the area of strong gradients as in the vicinity of the coastline (Fig. 3a). However, using model outputs at selected nodes for the depletion model requires water mass conservation along the *x*-axis used in the 1D model. Assuming that the variation in time of the water height is computed by the 2D

Table 1
List of equations for the ecophysiological model of scallop feeding and growth (from Hawkins et al., 2002)

Equations	Comments
Forcing functions	
PHYORG = CHL * chl2phy	Phytoplankton (mg l^{-1})
POM	Particulate organic matter (mg l^{-1})
TPM	Total particulate matter (mg l^{-1})
PIM	Particulate inorganic matter (mg l^{-1})
DETORG = POM - PHYORG	Detritus (mg l^{-1})
OCS = POM/TPM	Food organic content
TEMP	Temperature (°C)
State variables (initial value)	
TDW (0.116)	Tissue dry weight (g)
SDW (0.903)	Shell dry weight (g)
SEC (265)	Shell energy content (J)
TEC (2312)	Tissue energy content (J)
Parameters	
EDET = 6.1	POM energy content (J mg^{-1})
DW_standard = 1	Standardization weight (g)
Allo_feed = 0.62	Allometry coefficient for the ingestion
Allo_resp = 0.72	Allometry coefficient for the respiration
Energy_ratio = 0.897	Energy ratio between soft tissue and soft tissue plus shell energy
tissue2energy = 20	Tissue mass to energy conversion coefficient (J mg^{-1})
shell2energy = 0.294	Shell mass to energy conversion coefficient (J mg^{-1})
chl2phy = 0.1316	Chlorophyll to mass conversion coefficient (mg phyto µg $chla^{-1}$)
Filtration rate (mg d^{-1})	
Temp_lim = 2.751 * exp(- 0.00973 * (TEMP - 22.2).^2)	Temperature effect
allo_ir = (TDW/DW_standard) ** allo_feed	Allometry function
FRPHY = exp(2.598 + (5.88 * (log(log(POM) + 1))) + (3.56 * (log(POM) + 1)) + (0.406 * PHYORG)) * Temp_lim * allo_ir * 24	Phytoplankton
FRDET = (0.542 + 0.586 * DETORG) * Temp_lim * allo_ir * 24	Detritus
FRPOM = FRDET + FRPHY	POM
FRPIM = 19.06 * (1 - exp(- 0.110 * (PIM - 1.87))) * Temp_lim * allo_ir * 24	PIM
FRTPM = FRPHY + FRPIM + FRDET	TPM
PHYCNFPOM = FRPHY/FRPOM	Filtrated phytoplankton concentration
Rejection rate (mg d^{-1})	
RRFRPHYORG = 1.0 – (0.895 * PHYCNFPOM)	Phytoplankton enrichment factor
RRDET = – 0.00674 + (0.348 * FRDET)	Detritus
RRPHY = FRPHY * RRFRPHYORG	Phytoplankton
RRPIM = – 0.841 + 0.936 * FRPIM	PIM
RRTPM = RRDET + RRPHY + RRPIM	TPM
Ingestion rate (mg d^{-1})	
IRTPM = FRTPM - RRTPM	TPM
IRDET = FRDET - RRDET	Detritus
IRPHY = FRPHY - RRPHY	Phytoplankton
IRPIM = FRPIM - RRPIM	PIM
OCI = (IRDET + IRPHY)/IRTPM	Ingestion organic content
OIR = IRPHY + IRDET	Organic ingestion rate
Selection efficiency	
DETSEING = (IRDET/IRTPM)/(FRDET/FRTPM)	Detritus
PHYSEING = (IRPHY/IRTPM)/(FRPHY/FRTPM)	Phytoplankton
PIMSEING = (IRPIM/IRTPM)/(FRPIM/FRTPM)	PIM
Absorption rate (J d^{-1})	
NAEIO = 1.12 – 0.129 * 1/OCI	Net absorption efficiency
NEA = (23.5 * IRPHY + EDET * IRDET) * NAEIO	Net absorption rate
Respiration rate (J d^{-1})	
Temp_loss = exp(0.074 * TEMP)/0.33	Temperature effect
Maint_heat_loss = 3.55 * 24 * Temp_loss *	Maintenance
(TDW/DW_standard) ** allo_resp Total_heat_loss = 0.23 * NEA + Maint_heat_loss	Total respiration
Excretion rate (µg NH_4 d^{-1})	
O2N = 10 + 0.05 * NEA	Conversion from oxygen to nitrogen

Table 1 (continued)

Equations	Comments
Total_excr_loss = 62.23 * Total_heat_loss/NO$_2$	
Energy budget (J d^{-1})	
NEB = NEA - Total_heat_loss - Total_excr_loss * 0.02428	Net energy budget
Reproduction (J d^{-1})	
if (day.eq.165) then	Spawning at day 165 or 250
Reproduction = 0.07 * TEC	
Else	
if (day.eq.250) then	
Reproduction = 0.04 * TEC	
Else	
Reproduction = 0	
Endif	
Endif	Loss due to reproduction effort
if (NEB.lt.0) then	
Repro_loss = abs(NEB) + Reproduction	
Else	
Repro_loss = Reproduction	
Endif	
Net_loss = Repro_loss/tissue2energy/1000	Conversion from energy to mass
Scope for growth (J d^{-1})	
if (NEB.gt.0.and.TEC/(TEC + SEC).gt.Energy_ratio) then	SG = shell growth rate
SG = 0.103 * NEB	
Else	
SG = 0	
Endif	
if (NEB.gt.0) then	
if (TEC/(TEC + SEC).gt.Energy_ratio) then	TG = tissue growth rate
TG = 0.897 * NEB	
Else	
TG = NEB	
Endif	
Else	
TG = 0	
Endif	
Integration	Shell growth (g d^{-1})
Dshell = SG/shell2energy/1000	
Dtissue = TG/tissue2energy/1000	Tissue growth (g d^{-1})
TDW = TDW + (dtissue - Net_loss) * dt	dt = time step
SDW = SDW + (dshell) * dt	
SEC = SEC + (SG) * dt	
TEC = TEC + (TG - Repro_loss) * dt	

hydrodynamic and is uniform in space at the local scale, we wrote the same mass conservation equation as Roberts et al. (2000):

$$h \cdot \frac{\partial u}{\partial x} + \frac{\partial h}{\partial t} = 0 \qquad (3)$$

where h is the water height. The current velocity therefore varies in space and time.

2.2. Boundary conditions

Boundary conditions were needed to solve Eqs. (1)–(3). The hydrodynamic model yielded both sea level and current velocity required for Eq. (3). The current velocity was also measured at one site to check the validity of the model prediction. An Applied Microsystems EMP2000 electromagnetic current meter was moored 1 m below the surface in a cultivated area and current velocity and direction were recorded every minute for 15 d.

Time series were also needed for the environmental parameters. A monthly field survey was conducted between May 1999 and April 2000 at seven sites to measure the following parameters: temperature T, suspended particulate matter SPM, POM, particulate inorganic matter (PIM), and chlorophyll a CHL (Fig. 3a) (Hawkins et al., 2002).

These time series were used to compute food transport within the domain. In order to apply the depletion model to different sites of the bay, we interpolated the environmental parameters in space using the seven sampling stations and a linear interpolation method based on inverse distance weights. Though there was no obvious spatial gradient, we thought that mapping environmental parameters was the
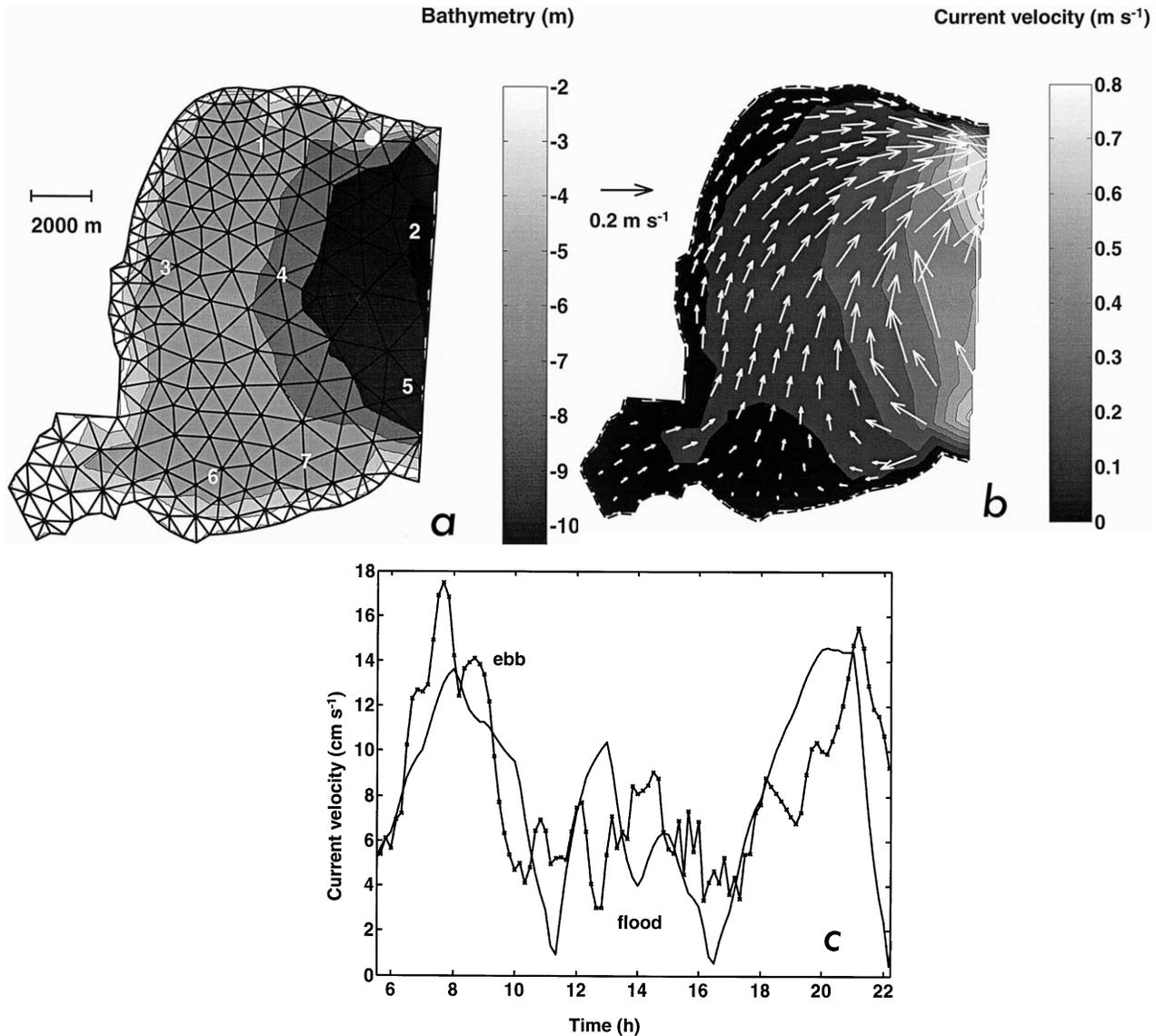
Fig. 3. Two-dimensional (2D) hydrodynamical model. (a) Grid used for the calculation of water height and current velocity and (from Grant and Bacher, 2001), location of sampling sites for the field survey (numbered from 1 to 7) and location of the continuous probe (white dot). (b) Current velocity field at one time of the tidal cycle and map of the maximum current velocity. (c) Current velocity measured in May 1999 compared to simulated values during one tidal cycle.

quickest and most relevant method to provide test values for the model at any location of the bay.

2.3. Simulations

Numerical integration of Eqs. (1)–(3) was based on discretization in space and time. The spatial domain was 1000 m and was split into three equivalently sized horizontal boxes to account for potential spatial variability, and the time step was equal to 600 s. The model was successively applied to all the nodes used by the hydrodynamical model (Fig. 3a) (149 nodes not counting the nodes at the terrestrial or oceanic boundaries). For each simulation, CHL, POM, PIM, individual scallop dry weight and total weight were computed for 1 year. Simulations started in October, which is the seeding

time (Hawkins et al., 2002). We therefore used our measured time series of SPM, POM, CHL, PIM, T to build annual forcing functions starting in October. Guo et al. (1999) describe the lantern net cultivation method in detail but, for our model, it is more relevant to consider the density of individuals (individuals per m^3). We tested two different densities: 0 and 50 ind m^{-3}. The null density refers to a case where we simulated the growth of a single individual without depletion and therefore provides the maximum annual weight. Comparing the two series of simulations allows the assessment of the density effect on the growth. After many sites with different hydrodynamic and food conditions were simulated, the results were mapped in order to assess the sensitivity of the density effect on the spatial variability of environmental conditions, as well as produce baywide patterns of seston
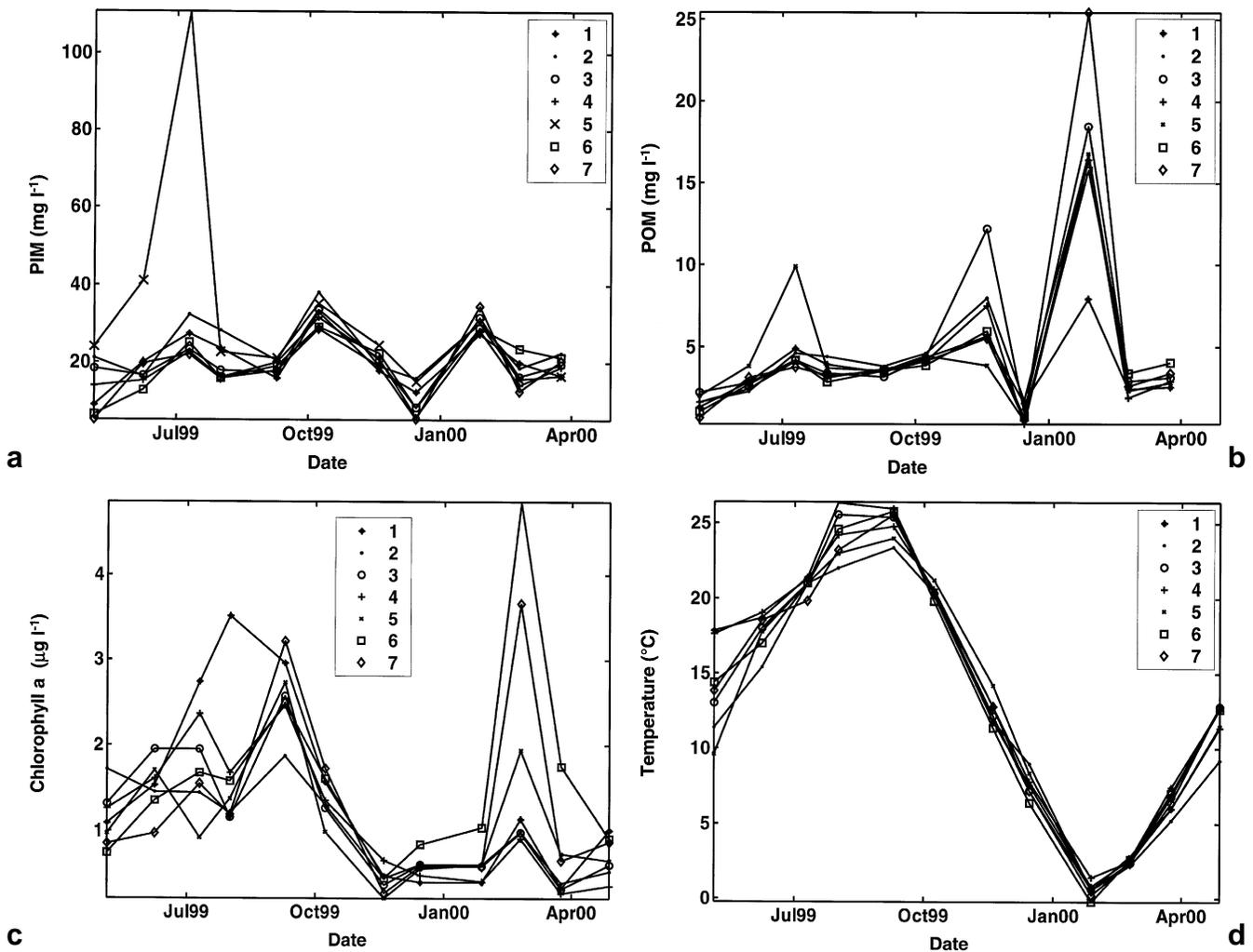
Fig. 4. Time series of environmental parameters measured from May 1999 to April 2000 at different sites. (a) PIM (mg l^{-1}). (b) POM (mg l^{-1}). (c) Chlorophyll *a* CHL (µg l^{-1}). (d) Temperature (°C).

3. Results

3.1. Field survey

The temperature of Sungo Bay oscillated between almost 0 °C in February 2000 and 26 °C in August 1999 with an average of ~14 °C (Fig. 4). The temperature was generally uniform among the seven sites, but large differences appeared in May 1999 and April 2000. For these dates, temperatures at sites 2 and 5 were lower compared to other sites, probably due to the more rapid warming of water masses in shallower waters. The mean chlorophyll *a* concentration was equal to 1.3 µg l^{-1}, with a maximum of five in February 2000. Concentrations were higher in spring and summer compared to winter—except for the peak in February. Peaks in Septem-

ber and February appeared simultaneously at all the sites, but in February, the peak was mainly located in the southern part of the bay (sites 5-7) with higher values inside the bay. However, no consistent spatial structure appeared in the chlorophyll *a* concentrations. The two highest values of TPM were greater than 40 mg l^{-1} and appeared in June and July at site 5—at the ocean boundary. The average TPM was ~22 mg l^{-1} with three peaks in July, October and January at all the sites simultaneously. The minimum values were ~6 mg l^{-1} and maximum values below 40 mg l^{-1} except for the two extreme values mentioned above. Some differences appeared between sites, especially in spring, but like chlorophyll *a*, no permanent spatial structure was detected. POM was correlated with TPM ($R = 0.43$, $P < 0.001$, $n = 77$) and the average POM/TPM ratio was ~0.20. POM concentrations were between 1 and 26 mg l^{-1}, with an average of 4.3 mg l^{-1} and the highest concentrations were measured in January. A weaker correlation existed between POM and chlorophyll *a* ($R = 0.22$, $P < 0.001$, $n = 77$).
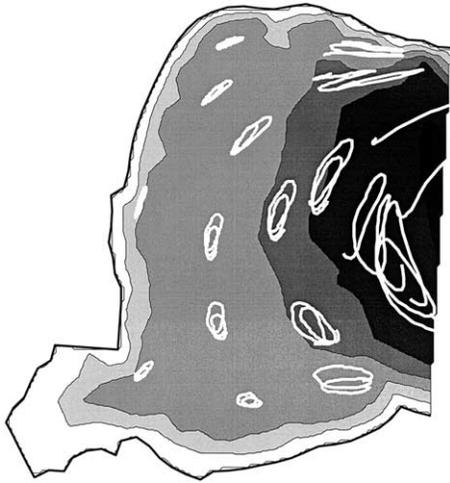
Fig. 5. The trajectory of particles during several tidal cycles predicted by the hydrodynamical model.

3.2. Hydrodynamics

Sungo Bay hydrodynamics are driven by tidal currents (Grant and Bacher, 2001). The amplitude of the water level variations was around 1 m and the relatively low current velocities were generated by the tidal amplitude (Fig. 3b). Computations showed that maximum current velocity occurred at the open boundary with the ocean, as opposed to the inner parts of the bay where maximum current velocity is usually less than 20 cm s^{-1}. Water circulation is dominated by a gyre due to the tidal phase in the open ocean (Grant and Bacher, 2001). During the flow, water enters the bay at the northeastern part of the ocean boundary and the tide reverses during the ebb. The residence time of water is around 20 d but computed trajectories showed that the daily displacement of particles was less than 2 km in the inner part of the bay (Fig. 5). Current velocity recorded in May 1999 was compared to simulated current velocityand both agreed reasonably well (Fig. 3c). The maximum current velocity was around 18 cm s^{-1} and ebb and flow were dissymmetric. However, measurements showed high variability when the current was low and at daily time scales (not shown), probably due to the influence of the wind which was not taken into account in the model.

3.3. Growth and depletion model

The growth model descrybed by Hawkins et al. (2002) was used to predict daily increases in scallop soft tissue weight over wide ranges of temperature, TPM, POM and chlorophyll a. First, the daily increase in tissue weight (SFG) was mapped against temperature (between 2 and 25 °C) and TPM (between 5 and 40 mg l^{-1}) (Fig. 6a). In a second series of calculations, SFG was mapped against POM (between 1 and 8 mg l^{-1}) and chlorophyll a (between 0.2 and 5 μg l^{-1}), at a constant temperature of 16 °C (Fig. 6b). For all these calculations, SFG increased from 0 to more than 30 mg d^{-1}. The results show positive effects of TPM and POM, with an

optimum temperature at 22 °C resulting largely from temperature limitations upon filtration rate (Table 1). The effects of temperature and TPM were combined; therefore the sensitivity of growth rate to TPM was enhanced when the temperature was between 20 and 25 °C. The effect of chlorophyll a concentration was smaller than POM. Chlorophyll a had a clear positive effect when POM was around 2 mg l^{-1}, but this effect nearly vanished for higher POM values, due to a lower contribution of phytoplankton to the food ration. Scallop growth was simulated from October 1999 to October 2000 using TPM, POM, temperature and chlorophyll a averaged over sampling sites (Fig. 6c). During this period of time, the scallop experienced two growth periods in autumn in relation to the high food concentrations and high water temperature. The dry weight was initially equal to 0.12 g and it reached a maximum of 1.6 g after 1 year. Scallops experienced a slight decrease in soft tissue weight due to very low temperature values in winter. One spawning occurred in June, which did not greatly affect the shape of the growth curve and the final weight.

Most findings related to food depletion were synthesized as maps of soft tissue weight at the end of annual simulations or of the seston depletion factor averaged over 1 year. These model outputs result from short-term variations of food concentration within the 1000 m long domain simulated by our depletion model. The domain was split into three boxes to account for spatial variability. One example of chlorophyll a variation during a single tidal cycle is shown in Fig. 7. In this simulation, scallop density was set to 50 animals m^{-3}, and scallop size to only 0.12 g, representing small animals. Results showed two oscillations per tidal cycle, with maximum concentrations in the upstream box (Box 1) when the inflow was highest and in the downstream box (Box 3) when flows were reversed. The greatest differences between boxes reached 20%, when the ratio between the maximum concentration and the mean concentration within the boxes was about 0.1.

Environmental parameters were interpolated in space and time, and the depletion model run successively for all nodes used in the hydrodynamic model (Fig. 3). The depletion model was first applied to compute annual scallop growth in the absence of any density or hydrodynamic effects, differences between sites being due to environmental conditions alone. The map of final tissue weights is shown in Fig. 8a. Values varied between 1.5 and 2.3 g; the most adequate areas being located around sites 3 and 5 of the field survey. Sites 1, 2, 6, 7 were less adequate, while site 4 was intermediary. A second series of simulations assessed the effects of a density of 50 ind m^{-3} (Fig. 8b), and the difference between the two scenarios is illustrated in Fig. 8c. Maximum values of about 2 g did not change much, but minimum values of about 0.8 g were much lower at these higher densities. Faster growth again occurred along the south oceanic boundary and in the vicinity of station 3, whereas slower growth became more obvious in the southwestern part of the bay. It is possible to compare the spatial variability of maximum current velocity
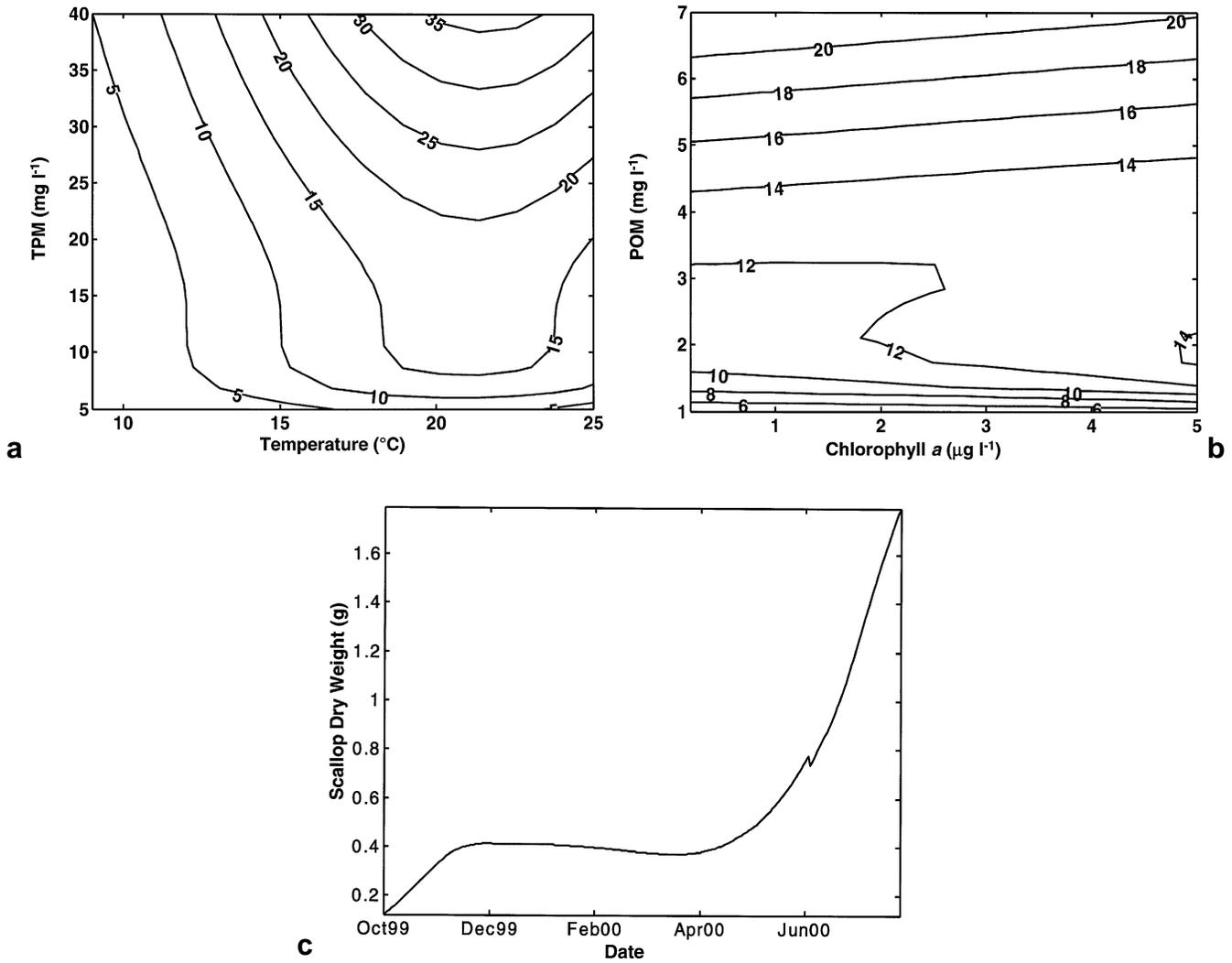
Fig. 6. Model prediction of scallop SFG. (a) SFG (mg d^{-1}) as a function of temperature (°C) and TPM (mg l^{-1}). (b) SFG as a function of chlorophyll a (μg l^{-1}) and POM (mg l^{-1}). (c) Simulation of scallop dry weight during 1 year based on TPM, POM, temperature and chlorophyll a averaged over different sites.
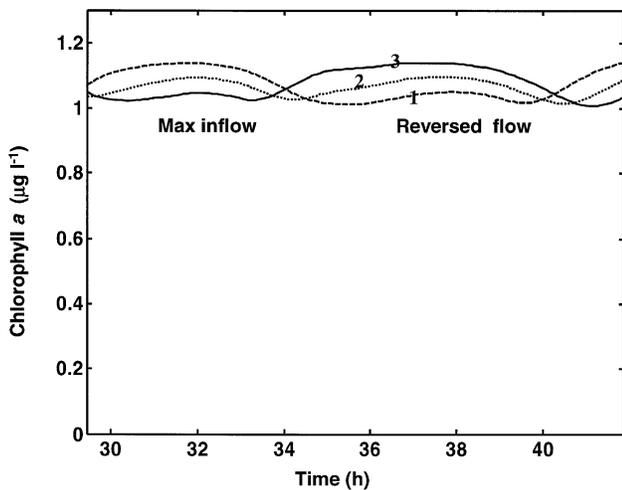
Fig. 7. Results of the depletion model: simulation of chlorophyll a CHL during one tidal cycle in three boxes.

(Fig. 3b) with localized predictions of scallop growth (Fig. 8a). When expressed as a percentage of final growth, the effects of density varied between 5% in the eastern part of the bay where the current velocity was strongest, to more than 30% in the southwestern part of the bay (Fig. 8c). Density effects of 10% or more occurred in 56% of the bay area.

The average POM depletion factor, defined as the ratio between the POM within the cultivated area and POM at the boundary averaged over boxes and time, was also mapped (Fig. 9a). Values varied between 0.75 and 0.95. Values close to 1 were found near the ocean boundary, and the southwestern part of the bay was characterized by the lowest depletion factor. In all the above calculations, depletion was due to ingestion of particles by scallops. Particles which were filtered but rejected as pseudofaeces prior to ingestion remained in the water column and could be utilized by scallops. When considering depletion in terms of scallop filtration, i.e. without accounting for pseudofaeces production, the density effect upon POM depletion was magnified; the maximum
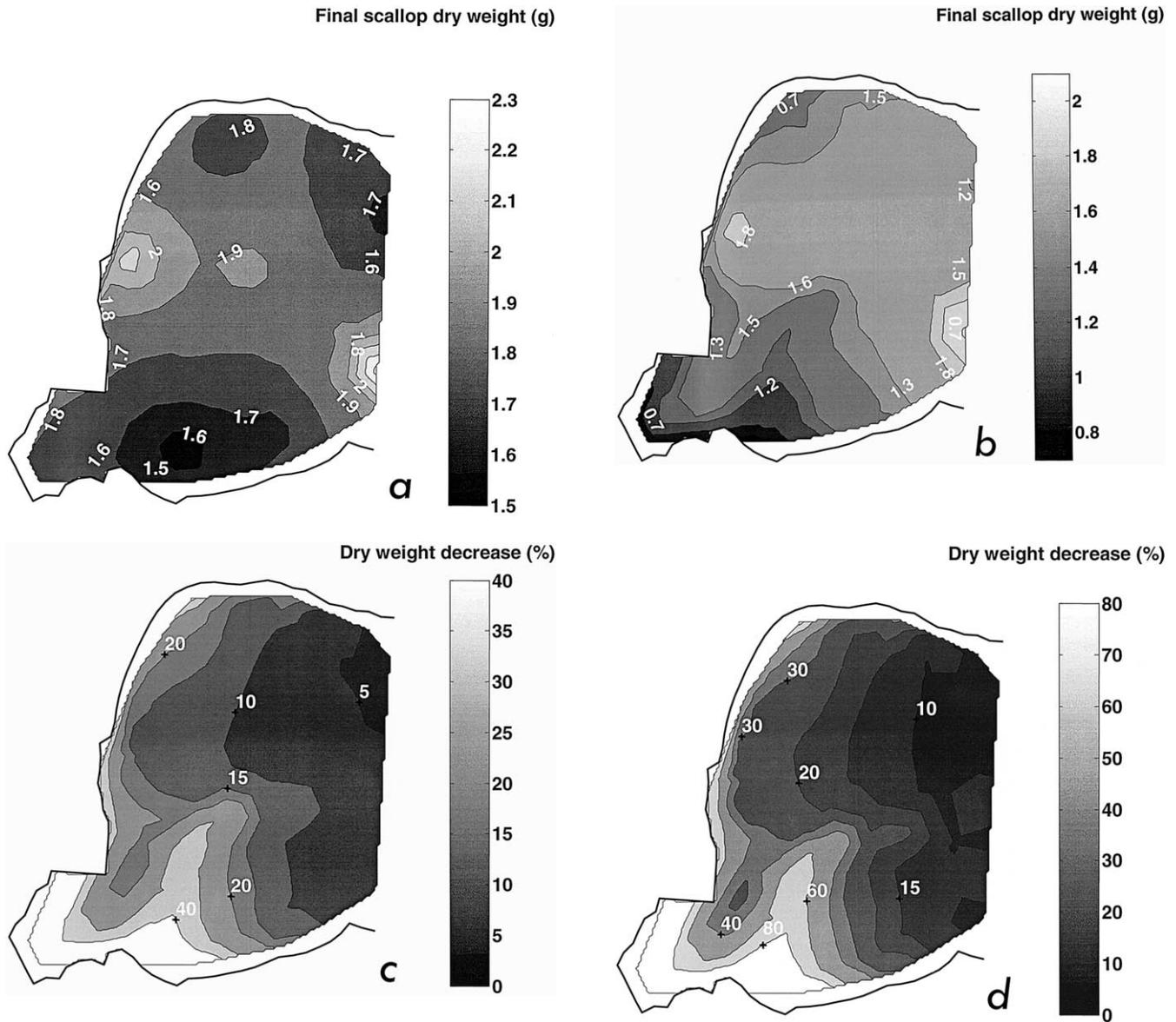
Fig. 8. Maps of the predicted effect of local density on scallop growth. (a) Map of annual scallop weight increase for a reference situation with no density effect. (b) Map of annual scallop weight increase for a constant density of 50 ind m^{-3}. (c) Sensitivity of scallop growth expressed as a percentage of annual growth variation between two simulations—null density, 50 ind m^{-3}. (d) Same as (c) when depletion was related to filtration instead of ingestion.

decrease in tissue weight reaching 80%, with a minimum depletion factor for POM of about 0.65 (Figs. 8 and 9). Final tissue weight, POM depletion factor based upon ingestion rates, maximum current speed are some of the model outputs at all nodes of the hydrodynamic model. In order to globally describe the relationships between these variables, final tissue weight was plotted against POM depletion factor (Fig. 10a), as well as against maximum current speed (Fig. 10b). The findings confirm a strong positive relation ($R^2 = 0.79$, $n = 149$) between depletion factor and final weight. They also indicate that final weight was strongly related to maximum current velocity when the latter was less than 0.2 m s^{-1} ($R^2 = 0.46$, $n = 113$), as opposed to higher speed values (Fig. 10b). The effect of current speed here was merely related to the

effect of scallop population on food concentration which was quantified by the depletion factor.

Since (i) density would affect individual growth, (ii) final weight is an objective of the farmer, and (iii) final weight is maximum with 0-density, we used the model to estimate densities that resulted in a given decrease in final tissue weight. We assumed a linear relationship between density and decrease in final weight and interpolated that decrease from previous simulations. We considered depletion based upon ingestion rate or filtration rate as discussed above, but illustrated that based upon ingestion alone here (Fig. 11). As an example, we chose a 10% decrease as an objective. In both the cases, densities were between 10 ind m^{-3} at sites where the density effect was the strongest and more than 100 in the
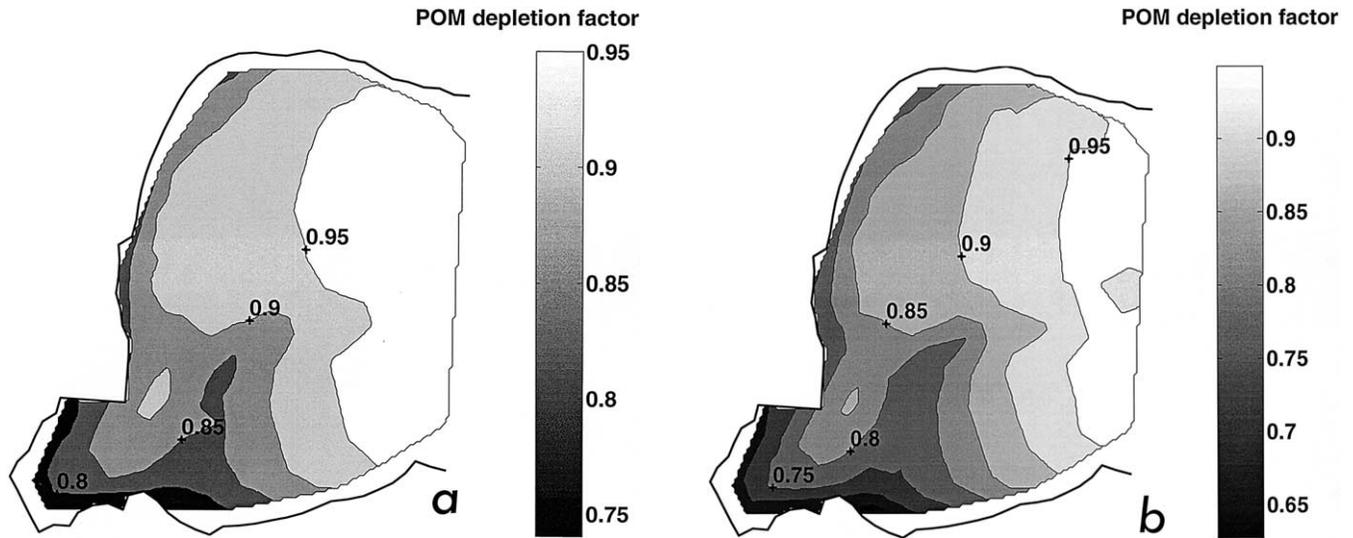
Fig. 9. Map of POM depletion factor with 50 ind m^{-3} averaged over 1 year. (a) Depletion due to ingestion rate. (b) Depletion due to filtration rate.

eastern part of the bay. When calculated for ingestion, thereby accounting for pseudofaeces reutilization, a density of less than 50 ind m^{-3} would be required over 67% of the bay to maintain a 10% weight decrease. This percentage would be 90% in case filtration was used in the calculation.

3.4. Modelling tool

A modelling tool was built to facilitate expertise on density dependent growth of scallops in Sungo Bay. This tool was based on the following components:

- Hydrodynamics were computed by Aquadyn© software (see Grant and Bacher, 2001), a Windows-based program that provides construction of the model finite element mesh as well as a hydrodynamic model (HydroSoft Energie, http://www.hydrosoftenergie.com). Outputs are saved in text files.

- Sungo Bay maps and database were implemented in a Geographic Information System with Arcview© software (ESRI, http://www.esri.com).
- Field data were stored in Barcawin© software (GEM, http://tejo.dcea.fct.unl.pt).
- The depletion model was developed in Fortran and Matlab computing language and compiled codes were interfaced with Arcview using Avenue© software.

The depletion model Graphical User Interface (GUI) helps the user to:
- plot current velocity and water height;
- compute and plot particle trajectories;
- select length scale, rearing density, site and simulate the annual scallop growth;
- map the final scallop growth or depletion factor;
- compare growth and depletion factors simulated with different densities on one site or over the bay;
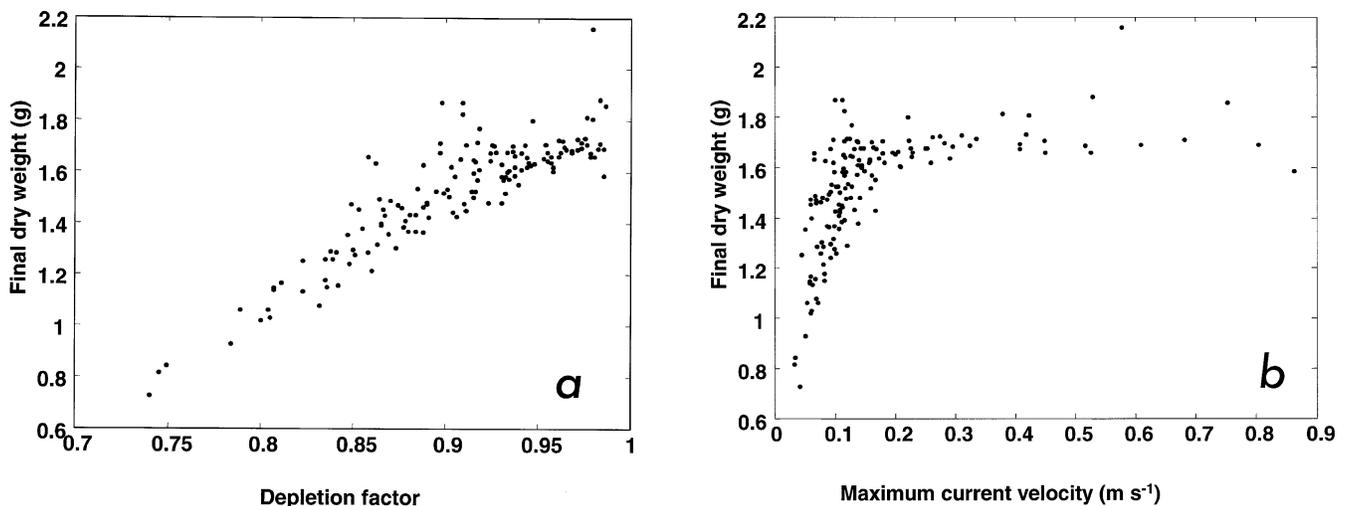
Fig. 10. Relationship between depletion factor, predicted final dry weight (g) and maximum current speed (m s^{-1}) plotted for all the nodes of the hydrodynamical model. (a) Plot of final weight vs. depletion factor. (b) Plot of final weight vs. maximum speed.
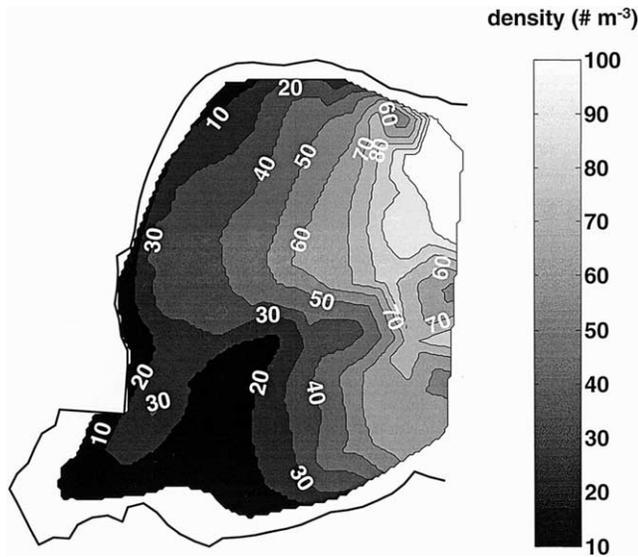
Fig. 11. Map of scallop rearing density according to 10% decrease of the final total weight.

- compute statistics of growth and depletion factors over the bay, such as the percentage of areas with a given depletion factor; and
- estimate the rearing density which guarantees a given depletion factor or a final scallop weight by simple arithmetics.

This tool provides information on suitable sites for scallop aquaculture, including appropriate local densities predicted on the basis of food depletion and limitation. All simulations and computations can be carried out within the GIS. When applied to one site, the time needed for a simulation of depletion and growth is less than a few seconds. When simulations are iterated for all the nodes of the hydrodynamical model, the total simulation time is only a few minutes.

4. Discussion

We have developed a depletion model coupling a detailed dynamic model of *C. farreri* feeding and growth and a 1D transport equation. The model was first applied to assess the effect of spatial variability in environmental parameters (e.g. TPM, POM, temperature, chlorophyll *a*) on growth. In the second step, effects of scallop density on growth through food depletion were simulated for a density of 50 ind m^{-3}. In all the simulations, food concentrations enabled a substantial weight increase to above 1.5 g dry soft tissues. The maximum growth difference due to differences between sites equalled 40%, and was mainly related to differences in POM, since temperature was homogeneous in space and net energy balance was influenced more by POM than by chlorophyll *a*. Scallop density had a clear net effect on growth at sites where maximum current velocities were below 20 cm s^{-1}. At greater current speeds, food renewal was always able to alleviate depletion. The percentage of variation in scallop growth that was due to density varied with the mean ratio between food available inside and outside the cultivated area (depletion factor). We also showed that scallop growth was correlated with maximum current velocity for a given density. Collective findings unequivocally establish that much of the variability in scallop growth resulted from food limitation.

Seston depletion has been addressed in various ways in previous studies, that include experimental approaches (Butman et al., 1994; Wildish and Kristmanson, 1984), field measurements (Pilditch et al., 2001; Roegner, 1998; Heasman et al., 1998; Fréchette et al., 1989) and models (Pilditch et al., 2001; Pouvreau et al., 2000; Campbell and Newell, 1998; Newell and Shumway, 1993; Bacher et al., 1997; Verhagen, 1982; Butman et al., 1994) (Table 2). Different types of depletion are considered. Most studies concern depletion at the benthic boundary layer, resulting from bot-

Table 2

Summary of published studies addressing the depletion issue. DW: dry weight; 2D: two-dimensional model

Density	Length	Current	Description	Reference
75 ind m^{-2}, 245 g DW m^{-2}	6 m	5–15 cm s^{-1}	Flume measurements, 2D vertical depletion model, benthic depletion	Butman et al. (1994)
500 g DW m^{-2} (0.3 g DW ind^{-1})	100 m	Max = 20 cm s^{-1}	Field measurements, 2D vertical depletion model, benthic boundary layer	Fréchette et al. (1989)
1400 g DW m^{-2}		5–50 cm s^{-1}	Seston depletion index (SDI), benthic boundary layer calculation	Wildish and Kristmanson (1997)
2000 g–11 000 g DW rope^{-1}, 700–3000 g DW m^{-3}	1200 m, 15 m	1.25–7.5 cm s^{-1}	Farm scale measurements, raft scale measurements	Heasman et al. (1998)
920 ind m^{-2}, 235 g DW m^{-2}	1000 m	Max = 35 cm s^{-1}	Field measurements, mass balance depletion model, benthic population	Roegner (1998)
0–50 ind m^{-3}, 0-50 g DW m^{-3}	1000 m	Max = 50 cm s^{-1}	Long lines, 1D depletion/growth model	This study
250–490 g DW m^{-2}	3.6 m	4–19 cm s^{-1}	Field flume	Wildish and Kristmanson (1984)
10–30 ind m^{-3}, 30-40 g DW m^{-3}	10 m	0.01–1 cm s^{-1}	1D depletion model	Pouvreau et al. (2000)
600 ind m^{-2}, 600 g DW m^{-2}	300 m	10 cm s^{-1}	1D vertical ecosystem model	Campbell and Newell (1998)
2 g DW m^{-3}	3000 m	1–15 cm s^{-1}	2D ecosystem model	Bacher et al. (1997)
2000 ind m^{-2}, 200 g DW m^{-2}	2000 m	5 cm s^{-1}	2D vertical depletion/growth model	Verhagen (1982)
250 ind m^{-2}	1000 m	5–30 cm s^{-1}	2D vertical depletion model	Newell and Shumway (1993)
12 ind m^{-3}, 120 g DW m^{-3}	80 m	Max = 5 cm s^{-1}	Long lines, measurements, 2D depletion model	Pilditch et al. (2001)

tom culture or benthic bivalve populations (Campbell and Newell, 1998; Newell and Shumway, 1993; Roegner, 1998; Verhagen, 1982; Butman et al., 1984; Wildish and Kristmanson, 1984, 1997). A few studies deal with cultivated species on rafts or long-lines (Bacher et al., 1997; Pouvreau et al., 2000; Heasman et al., 1998; Pilditch et al., 2001). Scales encompass a wide range of values. Lengths of the studied systems range from 6 m in experimental studies to more than 1000 m. For benthic populations, the density of studied systems ranges from 75 to 2000 ind m^{-2}, corresponding to ranges from 200 to 1 400 g soft tissue m^{-2}. For suspended cultures, the density of studied systems ranges between 2 and 700 g soft tissue m^{-3}. Minimum current velocities range from less than 1 to 35 cm s^{-1} (Table 2). All studies stress that food depletion may limit production, depending on the nature of the population (benthic, suspended), as well as scales of current velocity, density and length. Depletion would arise at spatial scales over a few kilometres when density is low or current velocity is high (Bacher et al., 1997; Newell and Shumway, 1993) and local depletion would not occur at smaller distances. Our calculations clearly confirmed the importance of depletion in the case of a bay with a large range of hydrodynamical conditions, at a scale of 1000 m and with a low density of animals. Our choice of 1000 m length stemmed from the mixing length defined from trajectory simulations. This guaranteed mixing of particles when water mass exited the 1000 m area, so that boundary conditions were correctly prescribed. Depletion would certainly occur at shorter lengths, but would be weaker unless densities are much higher, such as in raft culture (Heasman et al., 1998). For larger domains, we would have to consider other processes such as primary production, which would significantly compensate for the ingestion of particles by scallops. Here, we have demonstrated that managing rearing density at a 1000 m scale according to food supply and depletion alone provides useful indications on how to optimize individual growth.

Measuring food depletion, as well as its effect on growth and production, is problematic in the field. Fréchette et al. (1989) and Newell and Shumway (1993) demonstrated reduction in phytoplankton concentration near benthic boundary layers. In the water column, Ogilvie et al. (2000) assessed the effect of mussels on nutrients and chlorophyll *a* concentrations within farms, finding depletion when phytoplankton concentrations were low. Roegner (1998) measured food depletion in an estuary in some occasions though flux calculations always showed a significant effect of clearance rate due to benthic filter-feeders. Heasman et al. (1998) related differences in mussel growth to high depletion factors measured within densely cultivated rafts. Pilditch et al. (2001) did not observe reduction in seston concentration at a small scale, but expected a significant depletion if the lease area were to be extended. The reasons generally invoked for difficulty in measuring depletion are related either to scale (density, length, current velocity) or variability of environmental conditions. In the present study, it was quite clear that

environmental variability would mask the measurement of depletion in the field. Records of current velocity over several days were highly variable, probably due to the wind, with associated resuspension of organic and inorganic particles. On large scales, measurements of depletion would require intensive sampling in time and space, optimally using long-term moored instruments.

Several sources of uncertainty were apparent in our calculations. Measurements of current velocity revealed some variability, which would affect predictions of depletion and growth. However, hydrodynamics were dominated by the tide, which generated a regular and consistent pattern. More uncertainty is expected from the estimation of food availability. Previous studies (Fang, comm. pers.) showed that interannual levels of POM, TPM, and chlorophyll *a* have been changing over the past 20 years, probably due to changes in land use and aquaculture practices. Our sampling strategy based on a monthly field survey did not account for short-term variability related to tides, nor for changes in meteorological conditions on which information was lacking. We were forced to interpolate to supply sufficient data. Model outputs would certainly have benefited from a larger dataset, more accurately representing temporal and spatial variations of the forcing functions. Finally, outputs of the depletion model were sensitive to how we formulated the sink of particles, whether through ingestion, thus allowing for the reutilization of rejected matter, or through filtration, in which case, all the filtered particles were no longer available. Using ingestion minimized depletion, including effects of density on growth. It is likely that a significant fraction of pseudofaeces becomes available for reutilization following break up and resuspension. One way to resolve this uncertainty would be to measure the sinking rate of pseudofaeces in cultivated areas, and parameterize a biodeposition term in the depletion model.

Very high rearing densities would affect mortality and production (Fréchette et al., 2000), but we kept densities low enough in our calculations to assume no effect. We also assumed that primary production was negligible at the scale we chose. This can be acceptable when renewal time is short, which is presumably true in most parts of Sungo Bay. For instance, a 1000 m long domain is renewed every 3 h when the current speed is 10 cm s^{-1}. It can also be argued that phytoplankton is only a fraction of food ration and that neglecting phytoplankton production would not affect scallop growth. If really needed, source terms could, however, easily be added to Eq. (1) using phytoplankton turnover rates estimated from field measurements. Another potential improvement in our calculation concerns interactions between current velocity and filter-feeders, which were neglected. Grant and Bacher (2001), Boyd and Heasman (1998) and Pilditch et al. (2001) established that long lines or rafts modify the current velocity within cultivated areas, resulting in increased food depletion. In addition, Wildish and Kristmanson (1997) reported as to how scallop filter feeding may be inhibited at higher currents, though the effect of flow on

growth can be compensated when flow is periodic. Due to their complexity, both positive and negative effects are difficult to predict and have been neglected here, but we suggest that our predictions are a valid and quantitative approach for guiding aquaculture practice. From this perspective and to our knowledge, our model is the most spatially explicit with respect to modelling of density effects on aquaculture production ever attempted.

Our work was undertaken with the objective of helping to develop tools for the management of aquaculture. Campbell and Newell (1998) simulated local interactions between mussel beds and ecosystem processes, to provide recommendations on seeding density and timing. Pastres et al. (2001) also used a detailed ecosystem model to identify suitable sites for clam production in the lagoon of Venice. Other models have been developed to assess carrying capacity at the scale of the ecosystem (Raillard and Menesguen, 1994; Dowd, 1997; Bacher et al., 1998; Ferreira et al., 1998). A different approach was proposed by Arnold et al. (2000) to select lease sites for clam aquaculture in Florida, using multiple criteria based on the limitation of culture impact, water quality and associated spatial requirements. The novelty of our approach has been in coupling bivalve growth and food depletion at a site of intensive aquaculture, where identifying sustainable rearing densities is a major challenge. Food depletion factors, suitable rearing densities and expected individual growth rates can be superimposed with spatial information in a GIS, helping in the management of scallop aquaculture. Concepts (depletion), methods (coupling hydrodynamics and ecophysiology), and the underlying framework (GIS) are all generic, and can be applied to different sites where local interactions are important. Whilst of undoubted application at the farm scale, more comprehensive models will be required to simulate processes at larger ecosystem scales.

Acknowledgements

References

Arnold, W.S., White, M.W., Norris, H.A., Berrigan, M.E., 2000. Hard clam (*Mercenaria* spp.) aquaculture in Florida, USA: geographic information system applications to lease site selection. Aquacult. Eng. 23, 203–231.

Bacher, C., Duarte, P., Ferreira, J.G., Héral, M., Raillard, O., 1998. Assessment and comparison of the Marennes-Oléron Bay (France) and Carlingford Lough (Ireland) carrying capacity with ecosystem models. Aquat. Ecol. 31, 379–394.

Bacher, C., Millet, B., Vaquer, A., 1997. Modélisation de l'impact des mollusques cultivés sur la biomasse phytoplanctonique de l'étang de Thau (France). C.R. Acad. Sci. Paris, Sér. III 320, 73–81.

Barillé, L., Héral, M., Barillé-Boyer, A.L., 1997. Modélisation de l'écophysiologie de l'huître *Crassostrea gigas* dans un environnement estuarien. Aquat. Living Resour. 10, 31–48.

Boyd, A.J., Heasman, K.G., 1998. Shellfish mariculture in the Benguela system: water flow patterns within a mussel farm in Saldanha Bay, South Africa. J. Shellfish Res. 17, 25–32.

Butman, C.A., Fréchette, M., Geyer, W.R., Starczak, V.R., 1994. Flume experiments on food supply to the blue mussel Mytilus edulis L. as a function of boundary layer flow. Limnol.. Oceanogr. 39, 1755–1768.

Campbell, D.E., Newell, C.R., 1998. MUSMOD a production model for bottom culture of the blue mussel, *Mytilus edulis* L. J. Exp. Mar. Biol. Ecol. 219, 171–203.

Dame, R.F., 1993. Bivalve Filter Feeders in Estuarine and Coastal Ecosystem Processes. Springer-Verlag, 1993, Berlin, pp. 579.

Dowd, M., 1997. On predicting the growth of cultured bivalves. Ecol. Model. 104, 113–131.

Fang, J., Sun, H., Kuang, S., Sun, Y., Zhou, S., Song, Y., et al., 1996. Study on the carrying capacity of Sanggou Bay for the culture of scallop *Chlamys farreri*. Mar. Fish. Res. 17, 18–31 (in Chinese).

Ferreira, J.G., Duarte, P., Ball, B., 1998. Trophic capacity of Carlingford Lough for oyster culture—analysis by ecological modelling. Aquat. Ecol. 31, 361–378.

Fréchette, M., Butman, C.A., Geyer, W.R., 1989. The importance of boundary layer flows in supplying phytoplankton to the suspension feeder, *Mytilus edulis* L. Limnol. Oceanogr. 34, 19–36.

Fréchette, M., Gaudet, M., Vigneau, S., 2000. Estimating optimal population density for intermediate culture of scallops in spat collector bags. Aquaculture 183, 105–124.

Grant, J., 1996. The relationship of bioenergetics and the environment to the field growth of culture bivalves. Aquaculture 200, 239–256.

Grant, J., Bacher, C., 1998. Comparative models of mussel bioenergetics and their validation at field culture sites. J. Exp. Mar. Biol. Ecol. 219, 21–44.

Grant, J., Bacher, C., 2001. A numerical model of flow modification induced by suspended aquaculture in a Chinese bay. Can. J. Fish. Aquat. Sci. 58, 1003–1011.

Guo, X., Ford, S., Zhang, F., 1999. Molluscan aquaculture in China. J. Shellfish Res. 18, 19–32.

Hawkins, A.J.S., Duarte, P., Fang, J.G., Pascoe, P.L., Zhang, J.H., Zhang, X.L., et al., 2002. A functional simulation of responsive filter-feeding and growth in bivalve shellfish, configured and validated for the scallop *Chlamys farreri* during culture in China. J. Exp. Mar. Biol. Ecol. 281, 13–40.

Heasman, K.G., Pitcher, G.C., McQuaid, C.D., Hecht, T., 1998. Shellfish mariculture in the Benguela system: raft culture of *Mytilus galloprovincialis* and the effect of rope spacing on food extraction, growth rate, production, and condition of mussels. J. Shellfish Res 17, 33–39.

Incze, L.S., Lutz, R.A., True, E., 1981. Modelling carrying capacity for bivalve molluscs in open, suspended-culture systems. J. World Maricult. Soc. 12, 143–155.

Nath, S.S., Bolte, J.P., Ross, L.G., Aguilar-Manjarrez, J., 2000. Applications of geographical information system (GIS) for spatial decision support in aquaculture. Aquacult. Eng. 23, 233–278.

Newell, C.R., Shumway, S.E., 1993. Grazing of natural particulates by bivalves molluscs: a spatial and temporal perspective. In: Dame, R.F. (Ed.), Bivalve Filter Feeders in Estuarine and Coastal Ecosystem Processes. Springer-Verlag, Berlin, 1993, Berlin.

Ogilvie, S.C., Ross, A.H., Schiel, D.R., 2000. Phytoplankton biomass associated with mussel farms in Beatrix Bay, New Zealand. Aquaculture 181, 71–80.

Pastres, R., Solidoro, C., Cossarini, G., Melaku Canu, D., Dejak, C., 2001. Managing the rearing of *Tapes philippinarum* in the lagoon of Venice: a decision support system. Ecol. Model. 138, 231–245.

Pilditch, C.A., Grant, J., Bryan, K.R., 2001. Seston supply to sea scallops (*Placopecten magellanicus*) in suspended culture. Can. J. Fish. Aquat. Sci. 58, 241–253.

Pouvreau, S., Bacher, C., Héral, M., 2000. Ecophysiological model of growth and reproduction of the black pearl oyster, *Pinctada margaritifera*: potential applications for pearl farming in French Polynesia. Aquaculture 186, 117–144.

Powell, E.N., Hofmann, E.E., Klinck, J.M., Ray, S.M., 1992. Modelling oyster populations. I. A commentaryon filtration rate. Is faster always better? J. Shellfish Res. 11, 387–398.

Raillard, O., Deslous-Paoli, J.M., Héral, M., Razet, D., 1993. Modélisation du comportement nutritionnel et de la croissance de l'huître japonaise *Crassostrea gigas*. Oceanol. Acta 16, 73–82.

Raillard, O., Menesguen, A., 1994. An ecosystem box model for estimating the carrying capacity of a macrotidal shellfish system. Mar. Ecol. Prog. Ser. 115, 117–130.

Ren, J.S., Ross, A.H., 2001. A dynamic energy budget model of the Pacific oyster *Crassostrea gigas*. Ecol. Model. 142, 105–120.

Roberts, W., Le Hir, P., Whitehouse, R.J.S., 2000. Investigation using simple mathematical models of the effect of tidal currents and waves on the profile shape of intertidal mudflats. Cont. Shelf Res. 20, 1079–1097.

Roegner, G.C., 1998. Hydrodynamic control of supply of suspended chlorophyll a to infaunal estuarine bivalves. Estuar. Coast. Shelf Sci. 47, 369–384.

Scholten, H., Smaal, A.C., 1998. Responses of *Mytilus edulis* L. to varying food concentrations: testing EMMY, an ecophysiological model. J. Exp. Mar. Biol. Ecol. 219, 217–239.

Solidoro, C., Pastres, R., Melaku Canu, D., Pellizzato, M., Rossi, R., 2000. Modelling the growth of *Tapes philippinarum* in Northern Adriatic lagoons. Mar. Ecol. Prog. Ser. 199, 137–148.

Verhagen, J.H.G., 1982. A distribution and population model of the mussel *Mytilus edulis* in lake Grevelingen. Third International Conference on State-of-the-Art in Ecological Modelling, Colorado State University, May 24–28, 1982, pp. 373–383.

Wildish, D., Kristmanson, D., 1984. Importance to mussels of the benthic boundary layer. Can. J. Fish. Aquat. Sci. 41, 1618–1625.

Wildish, D., Kristmanson, D., 1997. Benthic Suspension Feeders and Flow. Cambridge University Press, 1997, New York.